Transient Algebraic Impedance Derivations and Applications for PLL-Synchronized IBRs

Lingling Fan, *Fellow, IEEE*, Zhixin Miao, *Senior Member, IEEE*,
Deepak Ramasubramanian, *Senior Member, IEEE*

***Abstract*—In system-level dynamic studies, grid-following inverter-based resources (IBRs) have been treated as current sources synchronized to the main grid via phase-locked-loops (PLL), while the interconnected transmission line is usually treated as a constant complex impedance. In this letter, we present the derivation of transient algebraic impedance of the transmission line and demonstrate its superiority over constant impedance. We show significant accuracy improvement in predicting transient stability and oscillations when the constant impedance is replaced by a transient algebraic impedance. Furthermore, we derive a small-signal model by use of the transient algebraic impedance and this model is successful in explaining the interaction between the PLL and the grid. On the other hand, if constant impedance is assumed, such stability issues cannot be predicted.**

***Index Terms*—Phase-locked loop, inverter-based resource, model reduction, stability analysis, nonlinear simulation**

I. Introduction

THE idea of transient algebraic circuit representation was introduced in 1993 by *Sauer et al.* in [1], in which the authors dealt with a synchronous generator and examined how synchronous generator's dynamics, e.g., speed deviation, may influence the voltage and current relationship of the interconnected transmission circuit. With flux being replaced by current, Sauer *et al.* were able to come up with a dynamic circuit representation relating the voltage and current phasors. In such a circuit, the derivative operator d/dt is kept. With this inclusion, the transmission line's reactance in the system DQ frame (rotating at the nominal frequency) is no longer a constant X, but rather $(1+v)X$ where v is a coefficient related to d/dt.

This expression of transient reactance is difficult to be understood. In our prior work, we have developed generalized dynamic circuits for a synchronous generator [2] operating at any speed and an unbalanced system [3] used operational calculus, or the Laplace transform variable s to substitute the derivative operator d/dt. The Laplace transform variable s has a clear physical meaning if viewed in the frequency domain. For example, in the system DQ frame with a constant rotating speed of ω_0, an inductance's impedance can be represented by $(s + j\omega_0)L$ [4], [5]. The operator s reflects the change of frequency during transients. Therefore, the reactance referred in [1] can be viewed in the frequency domain for elucidation.

This project is supported in part by NSF 2103480 and in part by EPRI grant 10014844. L. Fan and Z. Miao are with the Department of Electrical Engineering, University of South Florida, Tampa, FL, 33620 (e-mail: linglingfan, zmiao@usf.edu). D. Ramasubramanian is with EPRI (email: dramasubramanian@epri.com).

Demonstration in [1] is limited to one source case only where a generator is serving a load. Frequency in this type of islanding system is determined by the generator's speed solely. [1] has not shown how to implement transient algebraic impedance in a grid-connected system for demonstration since the implementation is not straightforward.

This paper aims to provide a thorough derivation and elucidation of transient algebraic impedance and further demonstrate its use in a grid-connected IBR system where the IBR is synchronized to the grid through PLL.

Transients in frequency may be inflicted by an IBR, which is usually viewed as a current source in the PLL frame. Therefore, if we want to include the effect of PLL dynamics, it seems intuitive to evaluate s by $j\Delta\omega$ where $\Delta\omega$ is the PLL's frequency deviation. The reactance of the line is therefore $(\omega_0 + \Delta\omega)L$. While a similar representation has been seen in the research on PLL related transient stability, e.g., [6], rigorous derivation of transient algebraic impedance in a grid-integrated PLL-synchronized IBR system has not been conducted in the current literature. Comparison against a testbed with grid EMT dynamics, along with the conventional reduced-order model, is also missing.

In this letter, we present rigorous derivations of transient algebraic impedance using two approaches: the ordinary differential equations (ODE) and the frequency-domain expressions (Section II). Furthermore, we implement transient algebraic impedance and explore two applications of high practical values. In Section III, we present the first application: model reduction for a grid-integrated IBR. This system is represented by an 8th-order model, while the reduced-order model has only 4 orders. In Section IV, we present the second application: stability analysis of PLL and grid interaction. Conclusion is presented in Section V.

II. Transient Algebraic Impedance Derivations

Assume a simple topology as shown in Fig. 1.

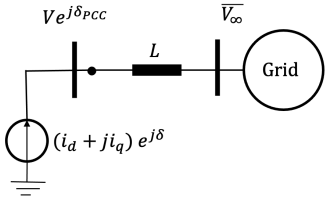

Fig. 1: A simple topology.

An IBR viewed as a constant current source (i_d+ji_q) in the PLL frame is interconnected to a constant voltage source $\overline{V}_\infty$ through a transmission line represented as a pure inductance.

The point of common coupling (PCC) bus voltage space vector viewed from the system DQ frame with a synchronous rotating speed ω_0 is notated as a complex vector or phasor $\overline{V} = Ve^{j\delta_{\rm PCC}}$ where V is the magnitude and $\delta_{\rm PCC}$ is the phase angle.

The current source assumption has been used extensively for reduced-order modeling [7], transient stability analysis [8], [9], etc. In [7], the line is assumed as a constant impedance.

A. Derivation based on ODE

In the system DQ frame, we may have the current source as $\overline{I} = (i_d + ji_q)e^{j\delta}$ and δ is the PLL output angle. PLL's main objective is to track the PCC bus voltage angle or to align its frame with the PCC bus voltage space vector. In the modeling and control perspective, the PCC bus voltage vector $\overline{V}$ is projected to the PLL frame (its angle against the system DQ frame is δ) and its q-axis component is enforced to be 0 at steady state. Fig. 2 shows the block diagram of a PLL viewed in the system DQ frame [10]. It can be seen that: $\frac{d\delta}{dt} = \Delta\omega, \quad \omega_{\rm PLL} = \omega_0 + \Delta\omega$.

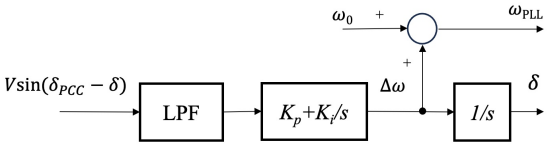

Fig. 2: PLL's control block diagram viewed from the system DQ frame. LPF stands for low-pass filter.

The relationship between the PCC bus voltage phasor and the current source is as follows:

$$\overline{V} = L\left(\frac{d}{dt} + j\omega_0\right)\overline{I} + \overline{V}_\infty \tag{1}$$

The complex vector based equation is viewed from the system DQ frame and this type of expressions can be found in classic books [11] and [12].

Let $\overline{I'} \triangleq i_d + ji_q$ as the current source viewed from the PLL frame, then $\overline{I} = \overline{I'}\, e^{j\delta}$. The derivative of $\overline{I}$ is expressed as follows.

$$\frac{d\overline{I}}{dt} = \frac{d\overline{I'}}{dt}e^{j\delta} + j\overline{I'}e^{j\delta}\cdot\frac{d\delta}{dt} \approx j\overline{I}\cdot\Delta\omega, \tag{2}$$

assuming that i_d and i_q are constants and $\frac{d\overline{I'}}{dt} \to 0$.

Therefore, (1) becomes the following:

$$\overline{V} = j\underbrace{(\omega_0 + \Delta\omega)L}_{X(\Delta\omega)}\,\overline{I} + \overline{V}_\infty, \tag{3}$$

The above equation shows that the voltage phasor and the current phasor are related by a *transient algebraic impedance.*

B. Derivation based on frequency domain expressions

Alternatively, we may examine the frequency-domain relationship between the PCC bus voltage $\overline{V}$ and the current phasor $\overline{I}$ in the system DQ frame:

$$\begin{aligned}\Delta\overline{V} &= (s + j\omega_0)L\cdot\Delta\overline{I} = (s + j\omega_0)L\cdot(\Delta\overline{I'}e^{j\delta} + j\overline{I}\Delta\delta)\\ &= j\omega_0 L\Delta\overline{I} + sL\Delta\overline{I'}e^{j\delta} + jL\overline{I}\cdot s\Delta\delta.\end{aligned} \tag{4}$$

It can be seen that three components contribute to $\Delta\overline{V}$.

1) When the transmission line is treated as a constant impedance, $\Delta\overline{V}$ has only the first component: $j\omega_0 L\Delta\overline{I}$.
2) The second component $sL\Delta\overline{I'}e^{j\delta}$ is due to the current transients. This component can be ignored since the constant current source is assumed due to very fast current control of IBR.
3) The third component $jL\overline{I}\cdot s\Delta\delta$ becomes algebraic (since $s\Delta\delta = \Delta\omega$): $jL\overline{I}\Delta\omega$.

Therefore, (4) becomes:

$$\Delta\overline{V} \approx j\omega_0 L\cdot\Delta\overline{I} + jL\overline{I}\cdot\Delta\omega = jL\Delta(\omega_{\rm PLL}\overline{I}) \tag{5}$$

Therefore, we may find the following:

$$\overline{V} = j\omega_{\rm PLL}L\cdot\overline{I} + \overline{V}_\infty = j(\omega_0 + \Delta\omega)L\cdot\overline{I} + \overline{V}_\infty. \tag{6}$$

Remark: The above derivation implicates that instead of ignoring all EMT dynamics of the transmission line, preserving part of them that is associated with PLL dynamics leads to a transient algebraic impedance.

III. Application 1: Dynamic Model Reduction

The test system is shown in Fig. 3. Compared to the circuit in Fig. 1, it has more sophistication by including not only series resistance but also a shunt capacitor. The RL circuit represents the transmission line, and the shunt capacitor represents shunt compensation. The synchronous reference frame-based PLL has a second-order low-pass filter, which is necessary for filtering out ripples caused by unbalanced input voltage [12]. The transfer function of the low-pass filter is as follows.

$$G_{\rm LPF} = \frac{\omega_f^2}{s^2 + 2\zeta\omega_f s + \omega_f^2}, \tag{7}$$

where $\zeta = 1$ and $\omega_f = 2\pi\times 25$ rad/s.

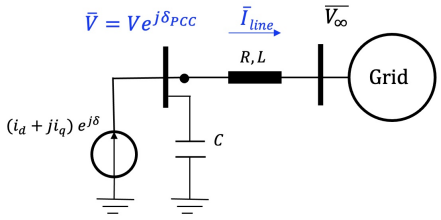

Fig. 3: The testbed for dynamic simulation.

In this study, two PLLs will be tested and they differ by their PI controller parameters. PLL1 has its proportional and integral gains at $(50, 500)$ while PLL2 has its gains at $(200, 2000)$. Based on the research carried out in [13], PLL2 is known to cause 20-Hz oscillations when the grid is weak.

The order of the EMT testbed (Model 1) in the system DQ frame is 8. State variables include the dq line current, dq PCC bus voltage, and 4 variables for the PLL (one related to the angle, one related to the frequency, and two related to the filter). Two reduced-order models are constructed, each having 4 orders. Model 2 uses transient algebraic impedance/admittance and therefore both the capacitor admittance and the inductor

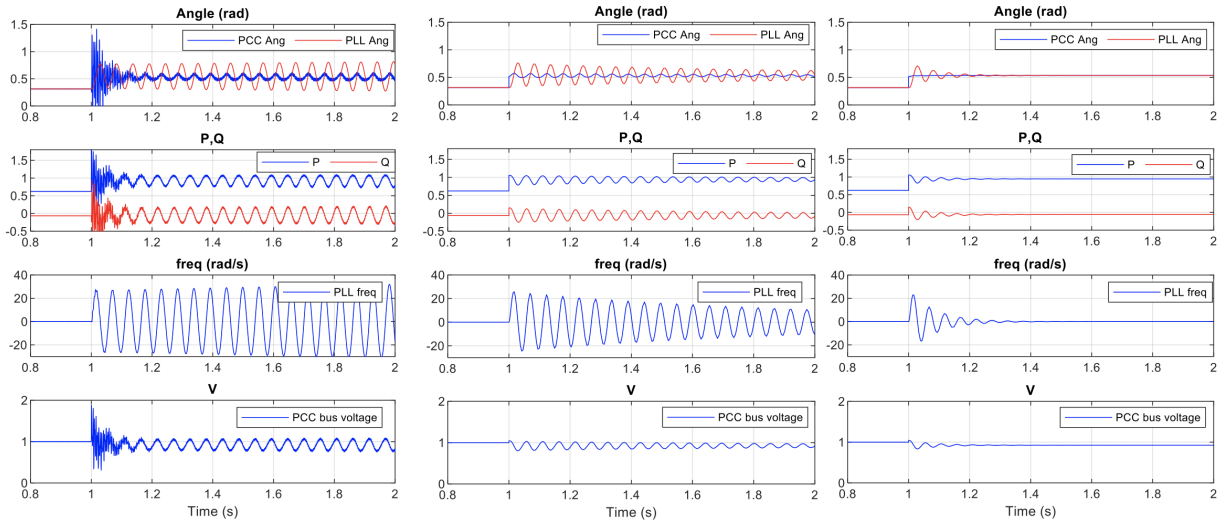

Fig. 4: Simulation results. $X = 0.5$, $B = 0.1$ and initial $i_d = 0.3885$ and $V = 1$. Left: Model 1. Middle: Model 2. Right: Model 3.

impedance contain transients related to the PLL frequency. The PCC bus voltage complex vector is related to the IBR current source and the grid voltage algebraically:

$$X = (\omega_0 + \Delta\omega)L, \quad B = (\omega_0 + \Delta\omega)C$$
$$\left(B + \frac{1}{R + jX}\right)\overline{V} = (i_d + ji_q)e^{j\delta} + \frac{\overline{V}_\infty}{R + jX}. \tag{8}$$

Model 3 has constant impedance and admittance. Table I presents the brief descriptions of the three models to be compared.

TABLE I: Comparison of Models

	comments	# of state variables
Model 1	EMT	8 (PLL, dq voltage, dq line current)
Model 2	transient algebraic impedance	4 (PLL)
Model 3	constant impedance	4 (PLL)

Fig. 4 shows the simulation results after 0.4 pu increase in i_d at $t = 1$ s, when PLL2 is employed. It can be clearly seen that Model 2 matches much better with Model 1. Model 2 can demonstrate the 20-Hz oscillations while Model 3 shows a very stable system.

In addition, an even larger increase in i_d is applied to examine the system behavior close to the transient stability margin when PLL1 is employed. Based on Fig. 5, Model 1 and Model 2 match very well while Model 3 shows a much more stable system.

Both simulation cases show that transient algebraic impedance leads to a much more accurate reduced-order model.

IV. Application 2: Small-Signal Stability Analysis

In this section, we explain why Model 2 can capture the 20-Hz oscillations while Model 3 cannot. Using the transient impedance, we develop a linear model to include PLL dynamics and the grid impact. In the following, we carry out stability analysis based on the transient impedance. We first

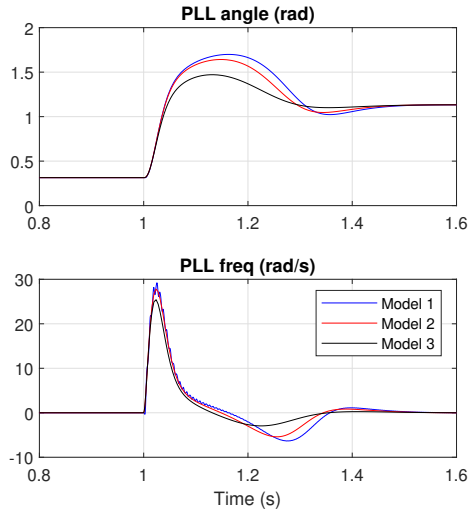

Fig. 5: Simulation results of i_d increases by 0.79 pu for a system with $X = 0.75; B = 0.1$. PLL parameters: (50, 500).

form a feedback system to describe the signal flow from δ_{PCC} to δ and back to δ_{PCC}.

Since a PLL tracks the PCC bus' phase angle δ_{PCC}, its closed-loop transfer function relates the PCC bus angle and the PLL angle. For a PLL with a low-pass filter, its closed-loop transfer function is as follows, assuming the voltage magnitude is 1 pu.

$$G_{\text{PLL}} = \frac{\Delta\delta}{\Delta\delta_{\text{PCC}}} = \frac{G_{\text{LPF}}\left(K_p + \frac{K_i}{s}\right)\frac{1}{s}}{1 + G_{\text{LPF}}\left(K_p + \frac{K_i}{s}\right)\frac{1}{s}}, \tag{9}$$

Next, the PCC bus' angle δ_{PCC} is influenced by the PLL angle δ through the transmission line circuit. A linear relationship between the PCC voltage phasor in the system DQ frame, and $\Delta\omega$ can be seen as follows:

$$\Delta\overline{V} = j\omega_0 L\Delta\overline{I} + j\overline{I}\Delta\omega L. \tag{10}$$

Note the above equation is a restatement of (5). Also note that if constant impedance is assumed and if the currents i_d

and i_q are constant, the voltage phasor and its angle show no influence towards the PLL frequency.

Let the system DQ frame align with the steady state PCC voltage space vector. Therefore, $\delta_{\text{PCC}} = \delta = 0$ and $\overline{I} = \overline{I'} = i_d + ji_q$ at steady state, and

$$\Delta\overline{V} = \Delta(Ve^{j\delta_{\text{PCC}}}) = \Delta V + jV\Delta\delta_{\text{PCC}}. \tag{11}$$

Similar small-signal expressions of the PCC bus voltage phasor in terms of its magnitude and angle can also be found in [7], [14].

For simplicity, assume that $i_q = 0$. Therefore, based on (10) and (11),

$$\begin{aligned} \Delta V &= -\omega_0 L \cdot \Delta i_q \\ V\Delta\delta_{\text{PCC}} &= Li_d \cdot \Delta\omega + \omega_0 L \cdot \Delta i_d \approx Li_d \cdot s\Delta\delta, \end{aligned} \tag{12}$$

by assuming $\Delta i_d \to 0$.

Note that this is a very important finding: The PCC bus' angle is proportional to the PLL frequency deviation.

The feedback system describing the relationship between the PCC voltage angle δ_{PCC} and the PLL angle δ is shown in Fig. 6.

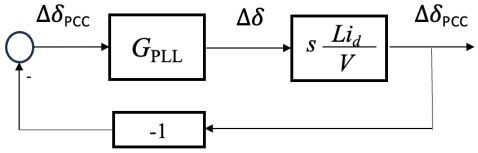

Fig. 6: The feedback system describing the PCC bus voltage angle and PLL angle relationship.

The loop gain of the feedback system is as follows:

$$\text{Loop Gain} = -\frac{\Delta\delta}{\Delta\delta_{\text{PCC}}}\frac{\Delta\delta_{\text{PCC}}}{\Delta\delta} = -G_{\text{PLL}}\frac{Li_d s}{V}. \tag{13}$$

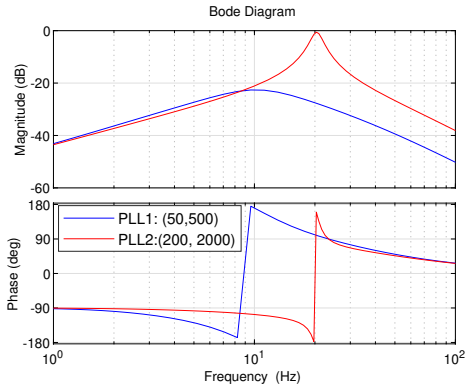

Fig. 7: The loop gain of the feedback system. $X = 0.5$ at the nominal frequency, $V = 1$ and $i_d = 0.7885$.

Fig. 7 shows the loop gain of the feedback system when $i_d = 0.7885$ and $X = 0.5$ pu. It can be seen that if PLL2 is used, the loop gain reaches 0 dB at the phase shifting frequency of 20 Hz. This indicates that the system is subject to 20-Hz oscillations. On the other hand, if PLL1 is used, the system is stable. The analysis results corroborate the simulation results based on Model 1 and Model 2 in Fig. 4.

If constant impedance is assumed, the PLL dynamics has no influence on the PCC bus angle. The system is always stable if G_{PLL} is stable. We no longer can explain this particular dynamic phenomenon which is influenced by grid impedance and exporting power level.

V. Conclusion

This letter offers a new perspective and method to incorporate IBR's influence into circuits. The essential technology is to preserve part of the circuit EMT dynamics that is associated with frequency or angle transients. This treatment is particularly useful to improve modeling accuracy for PLL-synchronized IBRs that can be viewed as current sources. This letter focuses on PLL's influence and this technology results in transient algebraic impedance, which further leads to reduced-order models suitable for nonlinear dynamic simulation and stability analysis. Compared with constant impedance, transient algebraic impedance helps detect interactions between PLLs and the grid and leads to more accurate dynamic performance without increasing the order of a model.

References

[1] P. Sauer, B. Lesieutre, and M. Pai, "Transient algebraic circuits for power system dynamic modelling," *International Journal of Electrical Power & Energy Systems*, vol. 15, no. 5, pp. 315–321, 1993.

[2] Z. Miao and L. Fan, "Generalized circuit representation for a synchronous machine," *IEEE Transactions on Energy Conversion*, vol. 38, no. 3, pp. 2235-2238, Sept. 2023.

[3] Z. Miao and L. Fan, "A Laplace-domain circuit model for fault and stability analysis considering unbalanced topology," *IEEE Transactions on Power Systems*, vol. 38, no. 2, pp. 1787–1790, March 2023.

[4] Z. Miao, "Impedance-model-based SSR analysis for type 3 wind generator and series-compensated network," *IEEE Transactions on Energy Conversion*, vol. 27, no. 4, pp. 984–991, Dec. 2012.

[5] Z. Miao, "Impact of unbalance on electrical and torsional resonances in power electronic interfaced wind energy systems," *IEEE Transactions on Powe Systems*, vol. 28, no. 3, pp. 3105–3113, Aug. 2013.

[6] Q. Hu, L. Fu, F. Ma, and F. Ji, "Large signal synchronizing instability of PLL-based VSC connected to weak ac grid," *IEEE Transactions on Power Systems*, vol. 34, no. 4, pp. 3220–3229, July 2019.

[7] L. Fan, "Modeling type-4 wind in weak grids," *IEEE trans. Sustainable Energy*, vol. 10, no. 2, pp. 853–864, April 2019.

[8] R. Ma, J. Li, J. Kurths, S. Cheng, and M. Zhan, "Generalized swing equation and transient synchronous stability with PLL-based VSC," *IEEE Transactions on Energy Conversion*, vol. 37, no. 2, pp. 1428–1441, June 2022.

[9] H. Geng, L. Liu, and R. Li, "Synchronization and reactive current support of pmsg-based wind farm during severe grid fault," *IEEE Transactions on Sustainable Energy*, vol. 9, no. 4, pp. 1596–1604, Oct.2018.

[10] L. Fan, *Control and dynamics in power systems and microgrids*. CRC Press, 2017.

[11] P. C. Krause, O. Wasynczuk, S. D. Sudhoff, and S. D. Pekarek, *Analysis of electric machinery and drive systems*. John Wiley & Sons, 2013, vol. 75.

[12] A. Yazdani and R. Iravani, *Voltage-sourced converters in power systems: modeling, control, and applications*. John Wiley & Sons, 2010.

[13] L. Fan *et al.*, "Real-world 20-Hz IBR subsynchronous oscillations: Signatures and mechanism analysis," *IEEE Transactions on Energy Conversion*, vol. 37, no. 4, pp. 2863–2873, Dec. 2022.

[14] L. Fan, Z. Miao, and M. Zhang, "Subcycle overvoltage dynamics in solar PVs," *IEEE Transactions on Power Delivery*, vol. 36, no. 3, pp. 1847–1858, June 2021.